Electronic Supplementary Material (ESI) for Journal of Materials Chemistry B.

Supporting Information

Enzyme-triggered on-demand release of H_2O_2-self-supplying $CuO_2@Fe_3O_4$ Nanoagent for enhanced chemodyamic antimicrobial therapy and wound healing

Sijie Zhang[a, b], Sameer Hussain[a], Yuhai Tang[a], Kaili Wang[b], Xingyan Wang[a], Long Zhang[b], Yuheng Liao[c], Chen Wang[c], Yi Hao[a, b*] and Ruixia Gao[a*]

[a]School of Chemistry, Xi'an Jiaotong University, Xi'an, Shaanxi 710049, China

[b]School of Pharmacy, Xi'an Jiaotong University, Xi'an, Shaanxi 710061, China

[c]Health Science Center, Xi'an Jiaotong University, Xi'an, Shaanxi 710061, China

Correspondence to: Yi Hao, E-mail: *haoyi8904@xjtu.edu.cn*

Prof. Ruixia Gao, E-mail: *ruixiagao@xjtu.edu.cn*

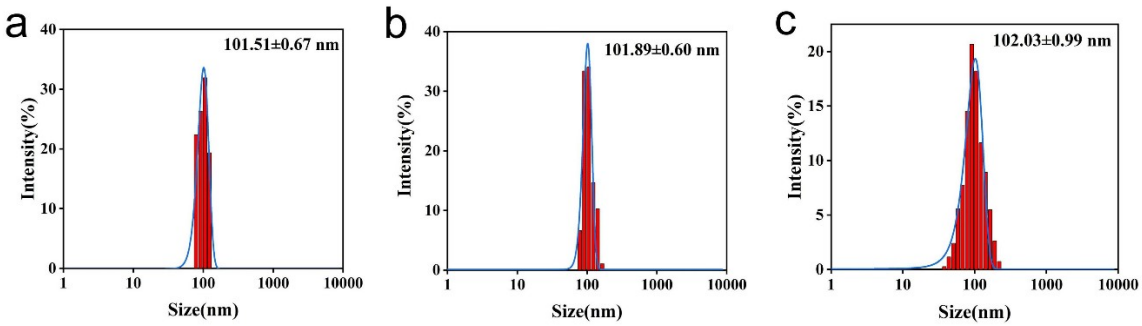

Figure S1. DLS size distribution of Fe_3O_4 (a), CP@Fe_3O_4 (b) and HA-CP@Fe_3O_4 (c).

a

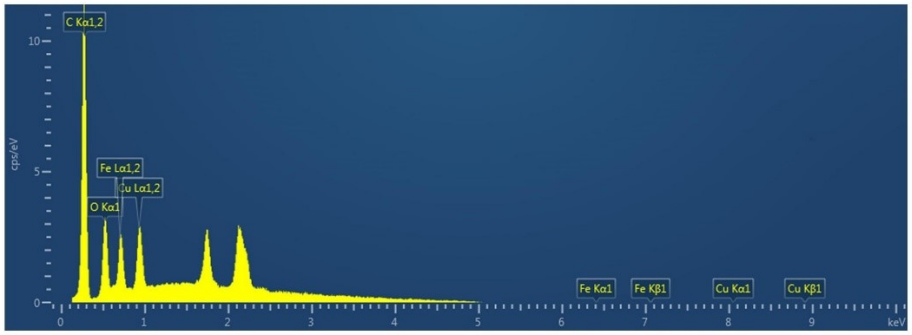

b

Element Line	Weight %	Weight % Sigma
C	45.0	0.5
Fe	29.7	0.6
Cu	17.0	0.4
O	8.2	0.2

Figure S2. Applying EDS for elemental analysis. A) Qualitative analysis: The peaks in the EDS spectrum represent C, Fe, Cu and O elements in HA-CP@Fe_3O_4. B) Quantitative analysis: Quantitative analysis is to obtain the content of C, Fe, Cu and O in HA-CP@Fe_3O_4 by X-ray intensity.

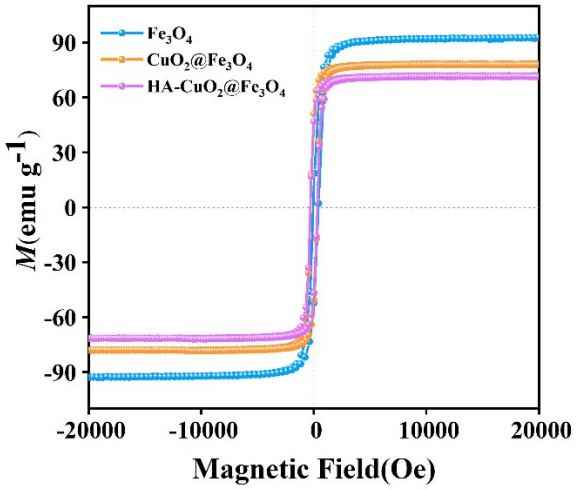

Figure S3. Room-temperature magnetic hysteresis loops of Fe_3O_4, CP@Fe_3O_4 and HA-CP@Fe_3O_4.

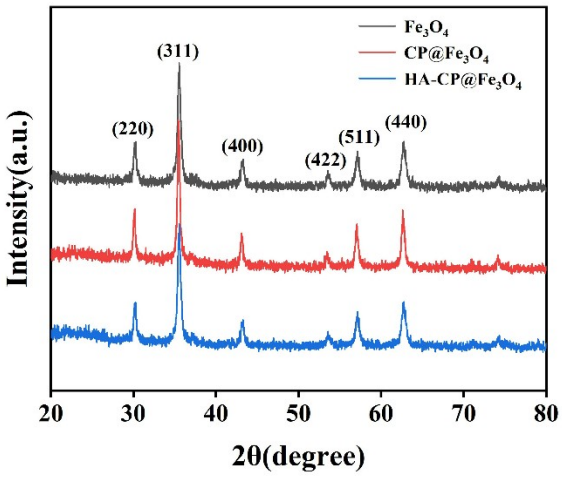

Figure S4. XRD patterns of Fe_3O_4 (black line) CP@Fe_3O_4 (red line) and HA-CP@Fe_3O_4 (blue line).

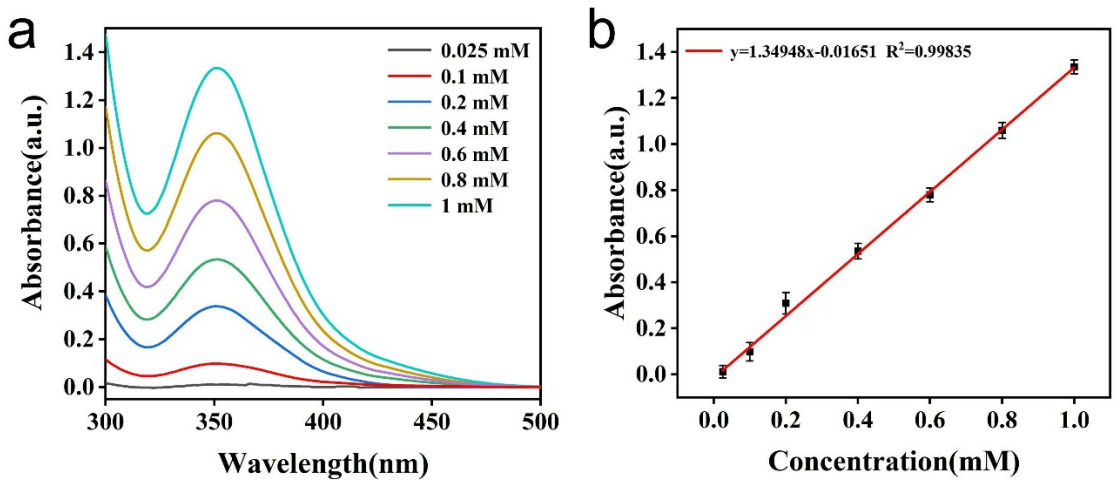

Figure S5. (a) The concentration of H_2O_2 was quantified by the absorbance of the product from the reaction of KI with H_2O_2. (b) Taking a fixed KI concentration as the reference, the absorbance was measured under different concentrations of H_2O_2 to obtain a calibration curve.

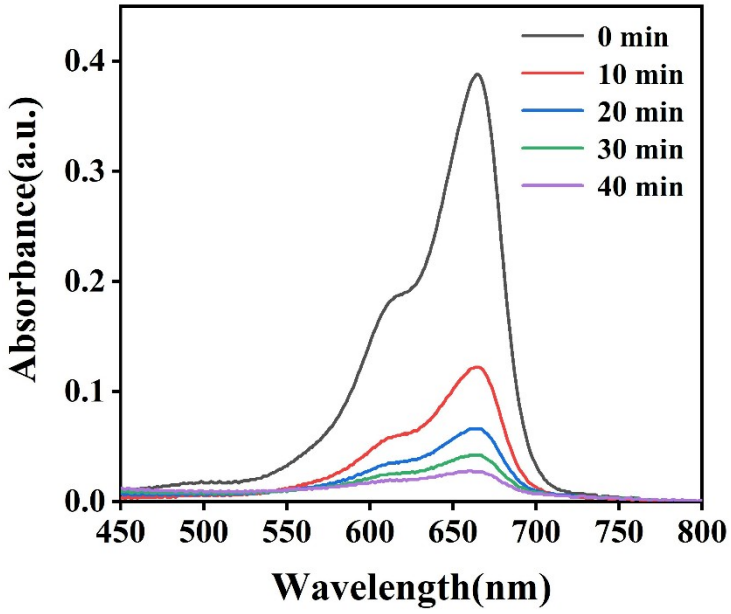

Figure S6. Absorption spectra of MB solution with HA-CP@Fe_3O_4 at increasing time intervals.

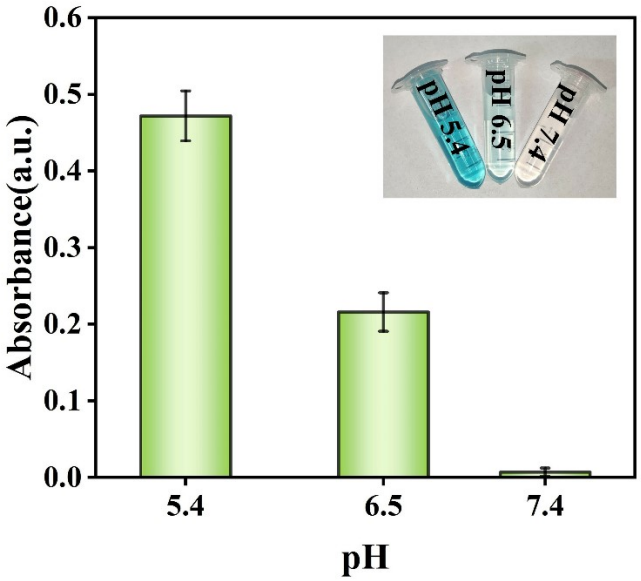

Figure S7. Fenton activity of HA-CP@Fe_3O_4 (200 μg/mL) at different pH after 60 min reaction.

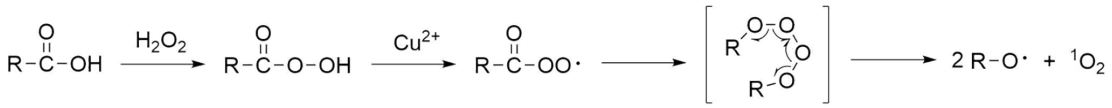

Figure S8. Russell reaction mechanism.

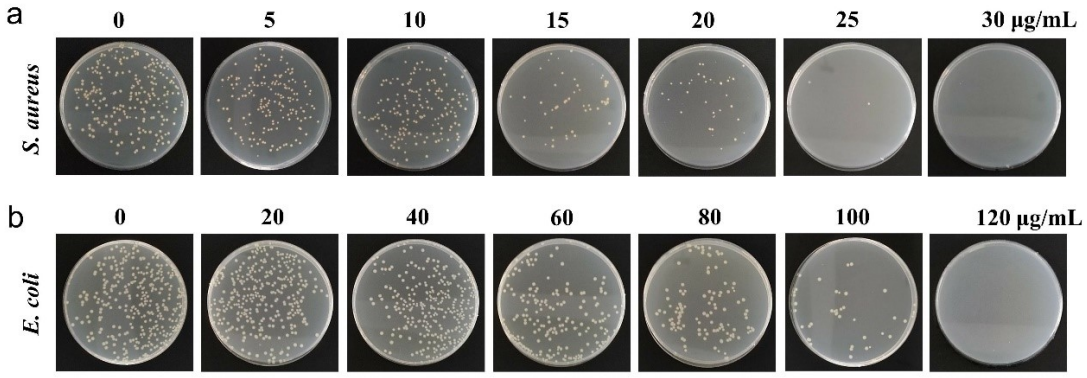

Figure S9. (a) Images of the LB agar plates of *S. aureus* treated with different concentrations of HA-CP@Fe_3O_4. (b) Images of the LB agar plates of *E. coli* treated with different concentrations of CP@Fe_3O_4.

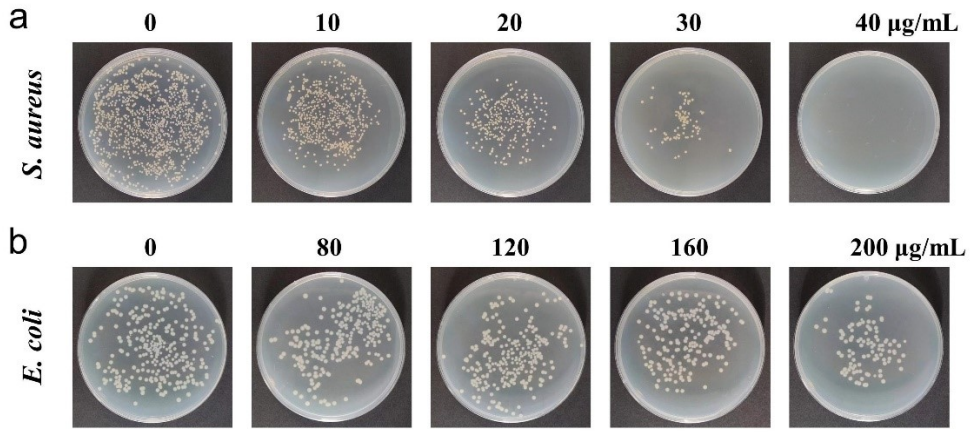

Figure S10. (a) Images of the LB agar plates of *S. aureus* treated with different concentrations of CP@Fe_3O_4. (b) Images of the LB agar plates of *E. coli* treated with different concentrations of HA-CP@Fe_3O_4.

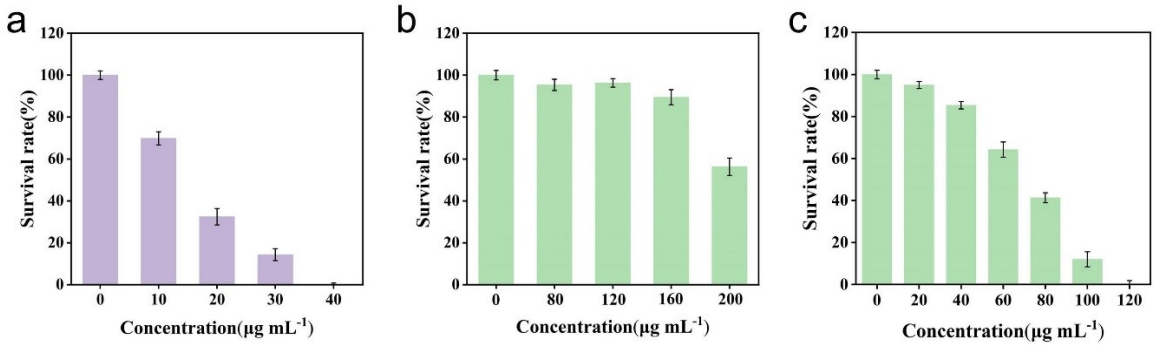

Figure S11. (a) Statistical analysis of *S. aureus* treated with different concentrations of CP@Fe_3O_4. (b) Statistical analysis of *E. coli* treated with different concentrations of HA-CP@Fe_3O_4. (c) Statistical analysis of *E. coli* treated with different concentrations of CP@Fe_3O_4.

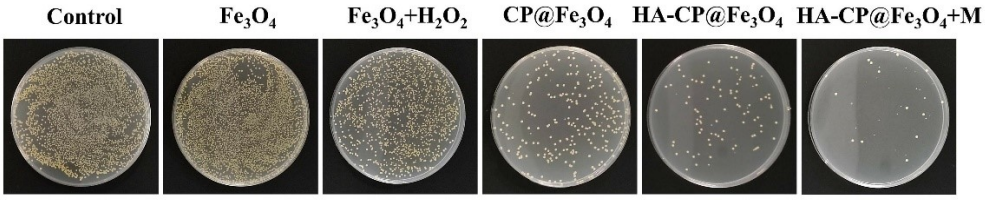

Figure S12. Bacteria isolated from wound tissue after different treatments were cultured on agar plates.

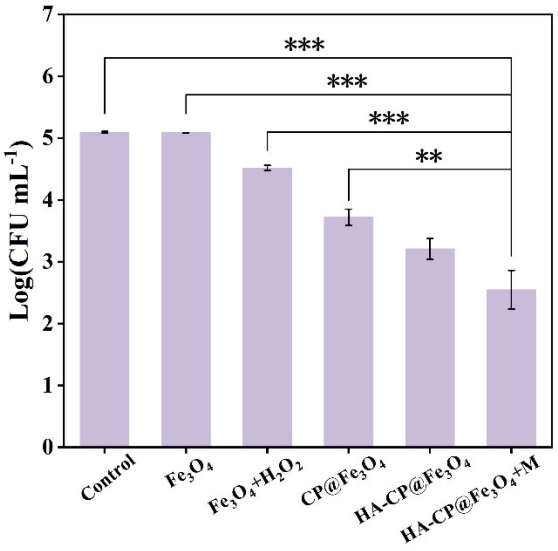

Figure S13. Bacterial viability from the infected wound tissues after treatment with different groups.

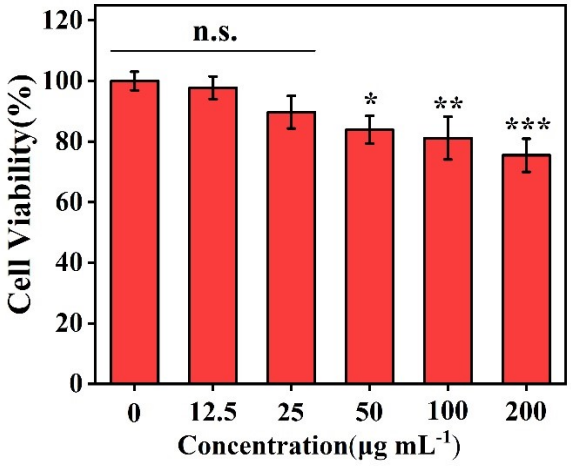

Figure S14. The survival rate of L929 cells after treatment with different concentrations of CP@Fe_3O_4 for 24 h.